Biochemical and Biophysical Research Communications 447 (2014) 358–363

Contents lists available at ScienceDirect

Biochemical and Biophysical Research Communications

journal homepage: www.elsevier.com/locate/ybbrc

Positive association of long telomeres with the invasive capacity of hepatocellular carcinoma cells

Eunkyong Ko, Guhung Jung *

Department of Biological Sciences, College of Natural Sciences, Seoul National University, 599 Gwanak-ro, Gwanak-gu, Seoul 151-747, South Korea

ARTICLE INFO

Article history:
Received 29 March 2014
Available online 13 April 2014

Keywords:
Telomere
Invasion
Telomerase reverse transcriptase (TERT)
Hepatocellular carcinoma (HCC)

ABSTRACT

Invasion, the representative feature of malignant tumors, leads to an increase in mortality. The malignant liver tumor – hepatocellular carcinoma (HCC) – has an enhanced invasive capacity that results in increased patient mortality. Moreover, this enhanced invasive capacity is due to the up-regulation of invasion promoters such as zinc finger protein SNAI1 (Snail) and matrix metalloproteinases (MMPs), and the down-regulation of invasion suppressor molecules such as E-cadherin. Telomerase reverse transcriptase (TERT), which encodes the catalytic subunit of telomerase, is highly expressed in a variety of invasive cancers, including HCC. Telomerase activation induces telomere elongation, thereby leading to cell immortalization during malignant tumor progression. However, the relationship between telomere length and invasion is yet to be experimentally corroborated. In this paper, we revealed that invasive HCC cells passing through the Matrigel display significantly longer telomeres than non-invasive HCC cells. Moreover, we established a method that can distinguish and sort cells containing long telomeres and short telomeres. Using this system, we observed that the HCC cells containing long telomeres had a high-level expression of invasion-promoting genes and a low-level expression of invasion-suppressing E-cadherin. Furthermore, HCC cells containing long telomeres exhibited a higher invasive capacity than HCC cells containing short telomeres. Taken together, our findings suggest that long telomeres are positively associated with the invasive capacity of HCC cells and may be a potent target for malignant liver cancer treatment.

© 2014 Elsevier Inc. All rights reserved.

1. Introduction

The acquisition of cellular immortality is a common occurrence in diverse cancers [1,2]. Telomere elongation is a prerequisite for the immortalization of cancer cells [1,3]. Telomerase facilitate the lengthening of telomeres, which are comprised of tandem repeats that contain a high number of T and G nucleotides at the chromosomal end [3,4]. Telomerase is composed of core components such as telomerase reverse transcriptase (TERT) and telomerase RNA (TERC) and accessory components such as DKC1, GAR1, NHP2, and NOP10 [5]. Among the telomerase components, TERT and TERC are necessary and required for the telomerase reconstitution [6,7].

Invasion is a primary cause of increased mortality in cancer patients [8,9]. Invasion-associated genes have been an active area of cancer research for the development and validation of essential drugs for cancer therapy [10–12]. Zinc finger protein SNAI1 (Snail), matrix metalloproteinases (MMPs), and E-cadherin are known to be important invasion-associated genes [13–15]. Notably, Snail accelerates tumor cell invasion via not only the down-regulation of E-cadherin but also up-regulation of the MMP family in HCC cell lines. The acceleration of tumor cell invasion is associated with poor prognosis for HCC patients [9,16].

Generally, an invasion assay using a Matrigel matrix is the assay of choice for detecting cell invasion in a cell culture system [13,14,17]. A Matrigel utilizes molecules such as laminin, collagen IV, and entactin to mimic the extracellular matrix and growth factors such as transforming growth factor-β (TGF-β), epidermal growth factor (EGF), insulin-like growth factor (IGF-1), and fibroblast growth factor (FGF) to enhance invasive ability [18]. The invasive capacity of cells can be determined by the number of cells that pass through the Matrigel matrix [16,18].

Telomerase is activated in 80–90% of tumors [19]. The canonical role of telomerase is to add telomeric DNA repeats for telomere elongation [20]. Moreover, the effects of silencing or overexpressing TERT on tumor cell invasion have been reported [20,21]. However, there have been no studies on the association between telomere length and invasion using a cell culture system. In this paper, we established a method for separating HCC cells containing long telomeres from HCC cells containing short telomeres. Furthermore,

* Corresponding author.
E-mail address: drjung@snu.ac.kr (G. Jung).

http://dx.doi.org/10.1016/j.bbrc.2014.04.022
0006-291X/© 2014 Elsevier Inc. All rights reserved.

we detected higher expression of invasion-promoting genes, lower expression of invasion-suppressing gene, and a higher invasive capacity in HCC cells with long telomeres than those with short telomeres. Thus, we expect that telomere elongation is essential for tumor cell invasion.

2. Materials and methods

2.1. Cell culture

HCC cells (Huh7 and Hep3B cells) were cultured in Dulbecco's modified Eagle's medium (DMEM, Welgene, Korea) supplemented with 10% fetal bovine serum (FBS, GenDEPOT, USA) and 1% antibiotics (Gibco, USA) in a humidified atmosphere at 37 °C and 5% CO_2 (NuAire Incubator, USA) [14].

2.2. Invasion assay and the collection of groups including non-invasive and invasive cells

Invasion assays were performed as described previously [14,17]. For the invasion assay, 5×10^4 cells were suspended in 300 μL of DMEM containing 0.1% bovine serum albumin (BSA) and loaded onto the upper compartment of a Transwell chamber that contained a Matrigel-coated polycarbonate membrane with a pore size of 8 μm pore size (BD Biosciences, USA). The cells that invaded through the Matrigel to the lower surface of the membrane were fixed using methanol and stained using crystal violet. The invaded cells were counted in three randomly selected microscopic fields of the fixed cells. The experiments were performed in triplicate.

For the collection of invasive and non-invasive cells, 5×10^5 cells were seeded in the upper compartment of a Transwell chamber that contained a Matrigel-coated polycarbonate membrane. Non-invasive cells were obtained from the cells in the Matrigel. The Matrigel was depolymerized by the addition of the BD Cell Recovery Solution (BD Biosciences). The invasive cells present on the lower surface of the membrane were obtained by the addition of Trypsin (Gibco).

2.3. Quantitative RT-PCR

Total RNA was isolated using the Ribozol RNA extraction reagent (Amresco) according to the manufacturer's protocol. Complementary DNA was synthesized from a total RNA of non-invasive and invasive cells using an AMV-Reverse Transcriptase kit (Promega). PCRs were performed using the QuantiTect SYBR Green PCR kit (Qiagen) and an ABI Prism 7300 Real-Time PCR System (Applied Biosystems). The primer sequences for each gene are indicated below: for TERT, forward (5′-GGAGCAAGTTGCAAAGCATTG-3′) and reverse (5′-TCCCACGACGTAGTCCATGTT-3′); for TERC, forward (5′-GGTGGTGGCCATTTTTTGTC-3′) and reverse (5′-CTAGAATGAACGGTGGAAGGC-3′); for DKC1, forward (5′-TGAAAAGGACCACATGGTGA-3′) and reverse (5′-TAATCTTGGCCCCATAGCAG-3′); for NHP2, forward (5′-GGTCAACCAGAACCCCATC-3′) and reverse (5′-GTGTCTCCTGCCAAAACCAT-3′); for NOP10, forward (5′-TACCTCAACGAGCAGGGAGA-3′) and reverse (5′- GGTCATGAGCACCTTGAAGC-3′); for GAR1, forward (5′-CAAGGACCTCCAGAACGTGT-3′) and reverse (5′-CCACTTTTCCAATTTGTTCTTTG-3′); for MMP7, forward (5′-TGCTGACATCATGATTGGCTTT-3′) and reverse (5′-TCCTCA TCGAAGTGAGCATCTC-3′); for MMP9, forward (5′-ATGCGTGGAGAGTCGAAATCTC-3′) and reverse (5′-GGTTCGCATGGCCTTCAG-3′); for Snail, forward (5′-TTCAACTGCAAATACTGCAACAAG-3′) and reverse (5′-CGTGTGGCTTCGGATGTG-3′); for E-cadherin, forward (5′-GTCATCCAACGGGAATGCA-3′) and reverse (5′-TGATCGGTTACCGTGATCAA AA-3′); for β-Actin, forward (5′-GCAAAGAC CTGTACGCCAACA-3′) and reverse (5′-TGCATCCTGTCGGCAATG-3′).

2.4. Telomere measurements

To measure telomere lengths, flow-FISH and immuno-FISH were performed as previously described with modifications [22,23]. For flow-FISH, cells were washed twice with PBS containing 0.1% w/v BSA. Subsequently, the cells were re-suspended in a hybridization buffer (70% deionized formamide [Amresco], 20 mM Tris–HCl [pH 6.8], 1% BSA, and 1 nM FAM-labeled 5′-$[TTAGGG]_3$-3′ peptide nucleic acid [PNA] probe [Panagene, Korea]). Next, the samples were incubated in an 85 °C water-bath for 10 min. After hybridization with the telomere probe in the dark at room temperature for 3 h, the samples were washed in each of washing solutions (washing solution I: 70% deionized formamide [Amresco], 10 mM Tris–HCl [pH 6.8], 0.1% BSA, and 0.1% Tween 20; washing solution II: 0.1% BSA and 0.1% Tween 20 in PBS) and incubated in a separate solution (0.1% BSA, 10 μg/mL RNase A, and 0.06 μg/mL 7-Aminoactinomycin D [7-AAD] in PBS) at 37 °C for 1 h. A total of 20,000 nuclei from each experimental group were analyzed. The telomere fluorescence intensity of the nuclei gated at the G1-G0 cell cycle stage was measured using a BD FACSCalibur flow cytometer (BD Biosciences) running on the CELLQUEST software.

For immuno-FISH, cells were fixed using 4% paraformaldehyde and subsequently dehydrated for 2 min each using 70%, 90%, and 100% ethanol. After drying in air, the cells were denatured using a hybridization solution (70% formamide in 2 × SSC, 5% $MgCl_2$, 0.25% blocking reagent [Roche], 12 nM Cy3-labeled 5′-$[CCCTAA]_3$-3′ PNA probe [Panagene], and 12.4 nM FAM-labeled centromere PNA probe [Panagene]) for 5 min at 85 °C. Subsequently, the cells were incubated in a humidified chamber for at least 2 h at room temperature. After hybridization, the cells were washed thrice for 15 min each in 70% formamide in 2 × SSC, washed in 2 × SSC twice for 10 min each, and finally washed in 0.1% Triton X-100 in PBS for 10 min. The cells were then mounted using mounting medium containing DAPI (Vector Laboratories). TFI/CFI refers to the ratio of telomere fluorescence intensity to centromere fluorescence intensity. A centromeric probe was used as an internal control. Images were obtained using a confocal microscope. Image analysis was performed using Image-Pro plus 6.0 software (Media Cybernetics).

2.5. Cell sorting according to telomere fluorescence intensity via flow cytometry

A Huh7 cell line stably expressing TPP1-GFP was established using 1 mg/mL of G418 selection antibiotic (Duchefa). The cells were dissociated at 37 °C in 0.2% w/v trypsin–EDTA (Gibco) for 10 min. After gentle pipetting to induce dissociation, the cells were washed twice with cold PBS containing 0.6% w/v BSA and filtered using a cell strainer (BD Bioscience). P3 cells displaying strong GFP expression and P4 cells displaying weak GFP expression were isolated from the stable Huh7 cell line expressing TPP1-GFP using a FACS Aria II (BD Bioscience).

2.6. Cell viability assay

The cell viability of Huh7 cells was measured by the 3-(4,5-dimethylthiazol-2-yl)-2,5-diphenyltetrazolium bromide (MTT, Sigma) assay. Ten thousand cells were seeded in 96-well plates. After 24 h incubation, cells were washed with PBS. And then, 180 μL of phenol red-free medium and 20 μL of MTT solution (5 mg of MTT/mL PBS) were added to each well. After 4 h incubation,

100 μL of DMSO was added and mixed thoroughly. The optical densities of formazan production were measured at 540 nm.

2.7. Flow cytometric analysis of cellular DNA contents

Two groups (P3 cells displaying strong GFP expression and P4 cells displaying weak GFP expression) were sorted by flow cytometry and were seeded in 60-mm dish. Cells were harvested at 24 h and 48 h by a trypsinization, centrifuged at 1000 rpm for 5 min, washed with cold PBS, and fixed overnight in 70% ethanol at 4 °C. Cells at 0 h were collected before cell seeding. Fixed cells were washed twice with PBS and incubated in PBS containing 0.1% BSA, 10 μg/mL RNase A, and 0.06 μg/mL 7-AAD at 37 °C for 1 h. Cell cycle profiles and cell population in G1, S, and G2/M phase were evaluated by BD FACSCalibur (BD Biosciences) using 7-AAD staining.

2.8. Statistical analysis

The data in the graphs are expressed as the means ± SD of three independent experiments. The statistical significance of the telomere measurements and the mRNA expression levels was evaluated using Fisher's exact test and a standard Student's *t*-test with a two-tailed distribution, respectively. Significance values were set at $^{*}p < 0.05$ and $^{**}p < 0.01$.

3. Results

3.1. Invasive HCC cells displayed significantly longer telomeres than the non-invasive HCC cells

To verify the correlation between telomere length and invasion in HCC cells, we collected non-invasive and invasive cells using a Matrigel invasion assay (Fig. 1A) and measured the telomere lengths of the cells via flow-FISH and immuno-FISH (Fig. 1B and C). The telomere lengths of the invasive cells were much longer than those of the non-invasive cells (Fig. 1B and C). The result showed a positive relationship between telomere length and invasion.

3.2. Invasive HCC cells displayed significantly higher TERT expression than the non-invasive HCC cells

To determine the mechanism by which telomeres are lengthened, we analyzed the mRNA expression levels of these telomerase components. The transcription levels of telomerase components, which include TERT, TERC, DKC1, GAR1, NHP2, and NOP10 (Fig. 2A) are positively associated with telomere-lengthening events [5]. Only the *TERT* mRNA levels were significantly higher in invasive HCC cells than in non-invasive HCC cells (Fig. 2B–G). These data suggest that the elevated levels of TERT expression contribute to the HCC cell invasion.

3.3. Invasive HCC cells displayed significantly higher invasion-promoting gene expression than non-invasive HCC cells

Quantification of the mRNA levels of invasion-promoting genes including *Snail*, *MMP7*, and *MMP9* is the primary method for testing whether invasive capacity is increased in HCC cells or HCC tumors [9,16,24,25]. While expression of the invasion-promoting genes *Snail*, *MMP7*, and *MMP9* was higher in invasive HCC cells than in non-invasive HCC cells (Fig. 3A–C), the expression of the invasion-suppressing *E-cadherin*, was lower (Fig. 3D). Therefore, we confirmed that invasive HCC cells have higher expression levels of invasion-promoting genes.

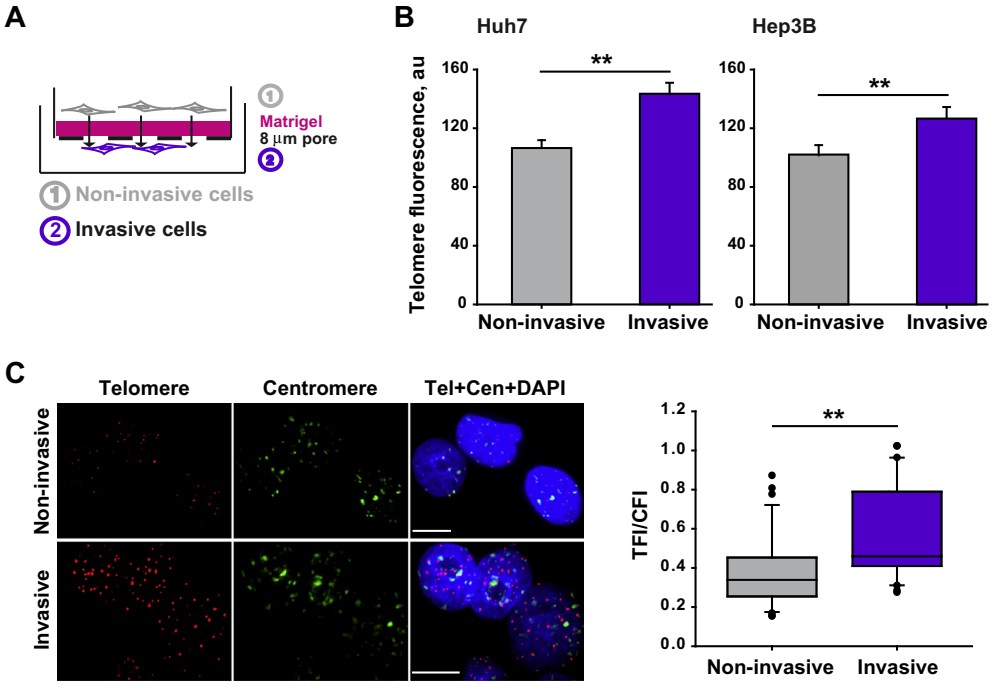

Fig. 1. Quantification of telomere lengths in non-invasive and invasive HCC cells. (A) Illustration of an invasion chamber composed of a Matrigel-coated Transwell insert. (B) Mean telomere measurement of non-invasive and invasive Huh7 cells (left) and Hep3B cells (right) via flow-FISH. Huh7 cells and Hep3B cells are HCC cells. au, arbitrary unit. (C) Immuno-FISH images of non-invasive and invasive Huh7 cells (left) and the quantification of telomere length in non-invasive ($n = 200$) and invasive Huh7 cells ($n = 220$) (right). Telomere (red), Centromere (green), and the DNA counterstain DAPI (blue). Telomere lengths were calculated by the ratio of telomere fluorescence intensity to centromere fluorescence intensity (TFI/CFI). The boxes illustrate the 25th to 75th percentile range. Horizontal bars inside the boxes indicate the median of telomere lengths. The whiskers above and below the box indicate the maximum and the minimum value of telomere lengths, respectively. Tel and Cen denote telomeres and centromeres, respectively. The scale bars, 10 μm. $^{**}p < 0.01$. (For interpretation of the references to color in this figure legend, the reader is referred to the web version of this article.)

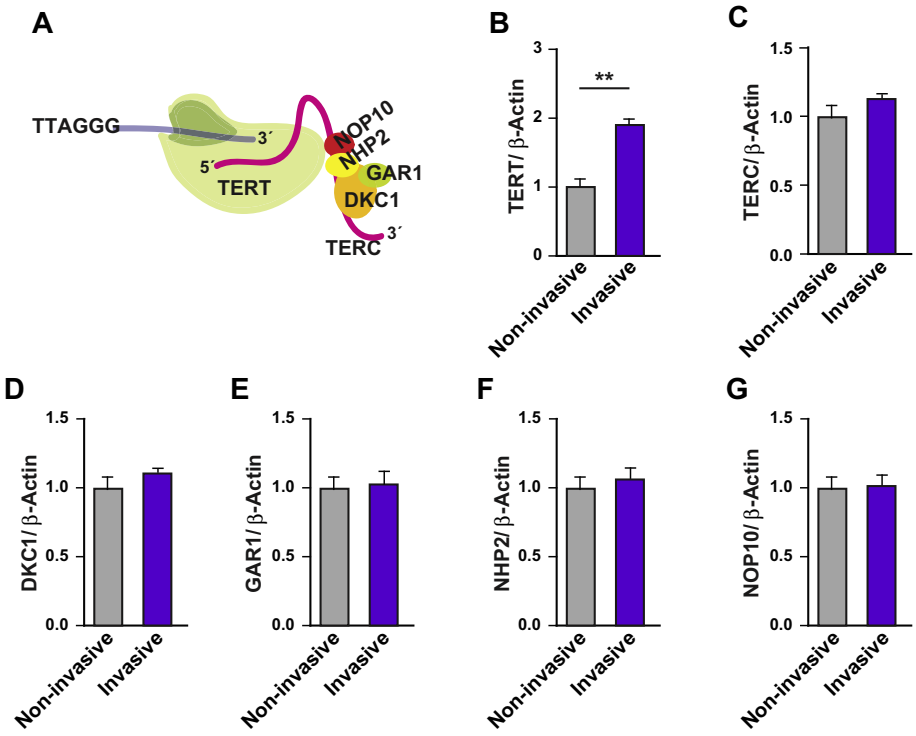

Fig. 2. Quantification of the mRNA levels of the telomerase components in non-invasive and invasive Huh7 cells. (A) The telomerase complex and its components. (B–G) mRNA levels of the telomerase components in non-invasive and invasive Huh7 cells. $^{**}p < 0.01$.

3.4. HCC cells containing long telomeres displayed significantly greater invasion than HCC cells containing short telomeres

Next, we investigated whether the cells containing long telomeres display higher expression of invasion-promoting genes and higher invasive capacity relative to cells containing short telomeres. To accomplish this, we established a stable Huh7 cell line expressing the telomere binding protein, TPP1 with GFP fusion [26]. A majority of the stable Huh7 cells showed TPP1-GFP localization to the nucleus and co-localization to telomeres (Fig. 4A and B). This allowed for the sorting of two groups by flow cytometry: one group of cells containing long telomeres and another group containing short telomeres. These groups were sorted according to the fluorescence intensity of TPP1-GFP (Fig. 4C). These two groups were similar with respect to cell viability, cell cycle profiles, DNA contents, and number of TPP1-GFP foci per cell (Fig. 4D–F).

Next, we examined the mRNA levels of invasion-associated genes by quantitative RT-PCR. We found that the higher expression of *Snail*, *MMP7*, and *MMP9* and the lower expression of *E-cadherin* were observed in HCC cells containing long telomeres when compared with HCC cells containing short telomeres (Fig. 4G). Finally, an invasion assay was performed to assess the influence of telomere length on the invasive capacity of the cells. We observed that HCC cells containing long telomeres exhibited a higher invasive capacity than the cells containing short telomeres (Fig. 4H). Therefore, we conclude that HCC cells containing long telomeres possess a higher invasive capacity and this may be attributed to the elevated expression of invasion-promoting genes and a reduction in *E-cadherin* expression.

4. Discussion

Along with an independent report that telomeres can be measured in living human cells via the CRISPR (clustered regularly interspaced short palindromic repeats)/Cas system [27], we measured telomere lengths of living cells via the quantification of fluorescence intensity of GFP fused to the telomere binding

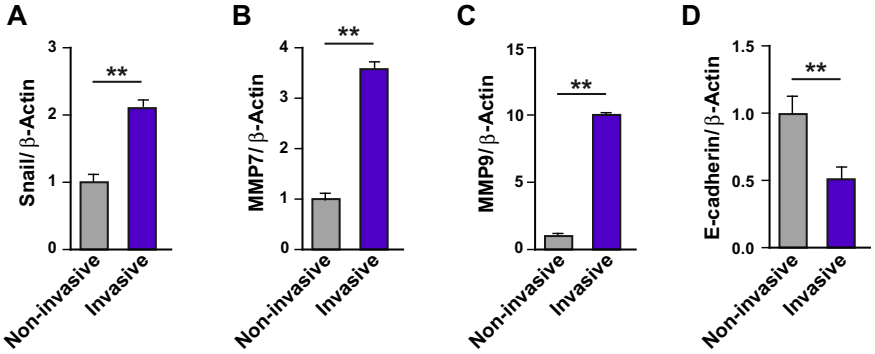

Fig. 3. Quantification of the mRNA levels of invasion-associated genes in non-invasive and invasive Huh7 cells. (A–D) mRNA levels of the invasion-associated genes in non-invasive and invasive Huh7 cells as measured by qRT-PCR. $^{**}p < 0.01$.

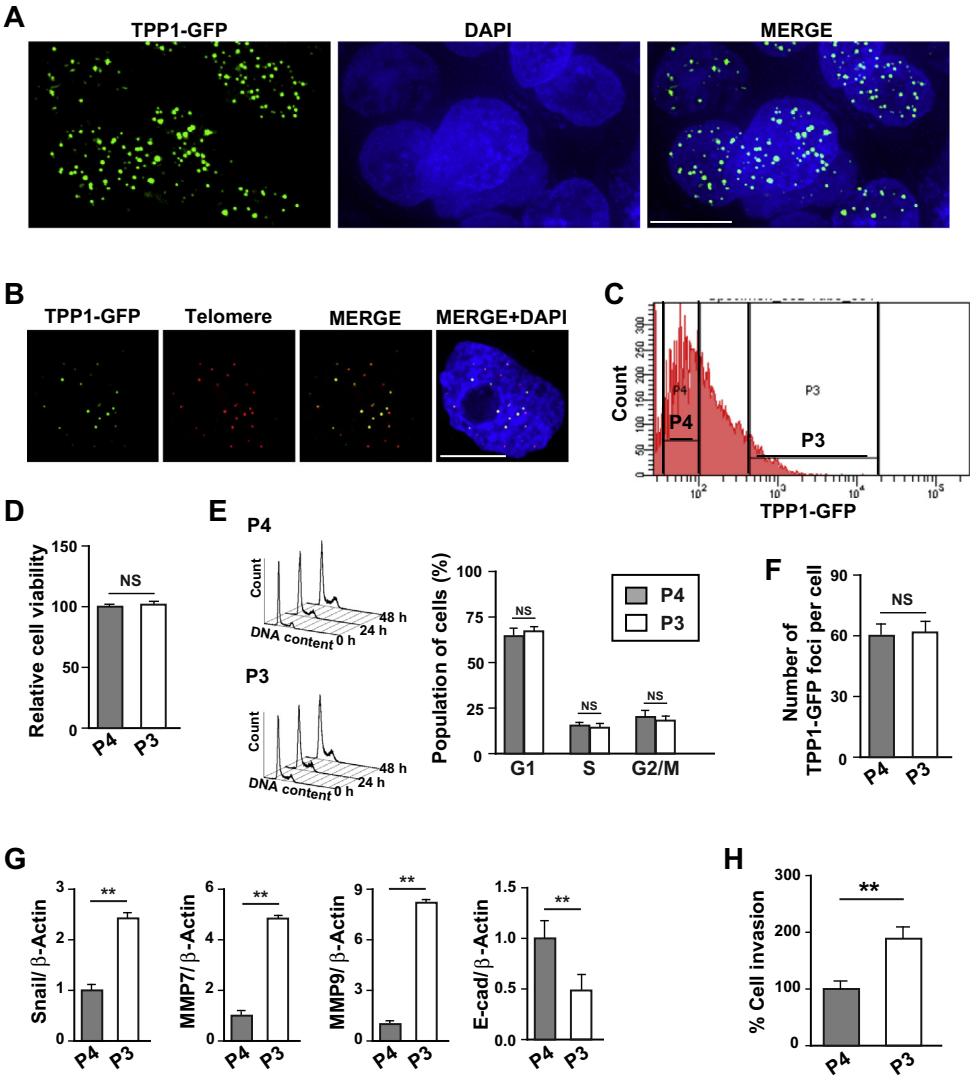

Fig. 4. Invasive capacity of Huh7 cells containing long telomeres and Huh7 cells containing short telomeres. (A) Fluorescence images of Huh7 cells stably expressing TPP1-GFP. Scale bars, 10 μm. (B) Immuno-FISH images from Huh7 cells stably expressing TPP1-GFP. TPP1-GFP (green), Telomere (red), and the DNA counterstain DAPI (blue). Scale bars, 10 μm. (C) Schematic image of the population with long telomeres (P3) and short telomeres (P4) in Huh7 cells. (D) Relative cell viability of the population with long telomeres (P3) and short telomeres (P4) in Huh7 cells. NS denotes non significance. (E) Analysis of cell cycle (left) and percentages of cells in G1, S, and G2/M phase (right) on the population with long telomeres (P3) and short telomeres (P4) in Huh7 cells. DNA contents at various times were analyzed by flow cytometry with 7-AAD staining. Forty-eight hours after cell seeding, percentages of cells were calculated. (F) Quantification of TPP1-GFP foci per cell of the population with long telomeres (P3) and short telomeres (P4) in Huh7 cells. Data are representative of three independent experiments ($n = 50$ cells analyzed per experiment). (G) mRNA levels of invasion-associated genes in Huh7 cells containing long and short telomeres. E-cad denotes E-cadherin. (H) Invasion assay using Huh7 cells containing long telomeres and short telomeres. $^{**}p < 0.01$. NS denotes non significance ($p > 0.05$). (For interpretation of the references to color in this figure legend, the reader is referred to the web version of this article.)

protein, TPP1 [26]. Baohui Chen et al. (2013) also shows that the similar values of telomere lengths are obtained by both quantification of the immunofluorescence intensity for endogenous telomere binding protein and the CRISPR/Cas system [27]. These results indicate that fluorescence-activating cell sorting via TPP1-GFP fluorescence intensity is a robust method for sorting cells based on telomere length. We separated the cell population containing long telomeres, which displays approximately the top 10% of telomere lengths from the overall cell population, based on the maximum value of invasive cells divided by the minimum value of non-invasive cells as a threshold. The cell population containing short telomeres exhibits the approximate bottom 10–50% range of telomere lengths. Based on the data derived from qRT-PCR and invasion assays (Fig. 4), the invasive capacity differs significantly between the cell population containing the top 10% of telomere lengths and the cell population containing the bottom 10–50% of telomere lengths. Thus, we conclude that the HCC cells containing long telomeres have an enhanced capacity for invasion.

Telomere elongation is responsible for cell immortalization [3,19]. Telomerase activation is primarily responsible for the lengthened telomeres present in malignant tumors [19,28,29]. We show that both telomere length and *TERT* mRNA levels are increased in invasive HCC cells when compared with non-invasive HCC cells (Figs. 1 and 2). *TERT* mRNA levels are very closely related to telomerase activity, as well as telomere length in diverse cancers, including HCC [28,29]. Thus, we suggest that long telomeres are associated with the up-regulation of *TERT* mRNA levels in invasive HCC cells.

Invasive Huh7 cells possess long telomeres and increased expression of invasion-promoting genes (Figs. 1 and 3). TERT is known to positively regulate Snail expression in gastric cancer cell lines [20]. Snail, one of the key regulators promoting invasion [9,16,30], increases *MMP7* mRNA levels in HCC cells [16]. Additionally, several reports have suggested that Snail may increase the MMP9 expression at both the mRNA and protein levels, leading to tumor cell invasion [30,31]. Moreover, Snail directly represses

the transcription of *E-cadherin* by binding to the *E-cadherin* promoter [14]. Therefore, we hypothesize that the up-regulation of TERT induces both the lengthening of telomeres and the up-regulation of invasion-promoting genes.

In summary, our data reveal that HCC cells containing long telomeres possess an enhanced invasive capacity. Long telomeres may serve as an important indicator for invasive HCC cells, thereby representing an essential therapeutic target for the prevention of malignant liver cancer.

Acknowledgments

This work was supported by Grants from the National Research Foundation of Korea (NRF), funded by the Korean government (MEST; No. NRF-2012R1A2A2A01047350).

References

[1] W.C. Hahn, S.A. Stewart, M.W. Brooks, S.G. York, E. Eaton, A. Kurachi, R.L. Beijersbergen, J.H. Knoll, M. Meyerson, R.A. Weinberg, Inhibition of telomerase limits the growth of human cancer cells, Nat. Med. 5 (1999) 1164–1170.
[2] H.B. El-Serag, K.L. Rudolph, Hepatocellular carcinoma: epidemiology and molecular carcinogenesis, Gastroenterology 132 (2007) 2557–2576.
[3] J.W. Shay, Determining if telomeres matter in colon cancer initiation or progression, J. Natl. Cancer Inst. 105 (2013) 1166–1168.
[4] T. von Zglinicki, Oxidative stress shortens telomeres, Trends Biochem. Sci. 27 (2002) 339–344.
[5] T. Vulliamy, R. Beswick, M. Kirwan, A. Marrone, M. Digweed, A. Walne, I. Dokal, Mutations in the telomerase component NHP2 cause the premature ageing syndrome dyskeratosis congenita, Proc. Natl. Acad. Sci. U.S.A. 105 (2008) 8073–8078.
[6] T.M. Bryan, T.R. Cech, Telomerase and the maintenance of chromosome ends, Curr. Opin. Cell Biol. 11 (1999) 318–324.
[7] S.L. Weinrich, R. Pruzan, L. Ma, M. Ouellette, V.M. Tesmer, S.E. Holt, A.G. Bodnar, S. Lichtsteiner, N.W. Kim, J.B. Trager, R.D. Taylor, R. Carlos, W.H. Andrews, W.E. Wright, J.W. Shay, C.B. Harley, G.B. Morin, Reconstitution of human telomerase with the template RNA component hTR and the catalytic protein subunit hTRT, Nat. Genet. 17 (1997) 498–502.
[8] P. Kelly, L.N. Stemmle, J.F. Madden, T.A. Fields, Y. Daaka, P.J. Casey, A role for the G12 family of heterotrimeric G proteins in prostate cancer invasion, J. Biol. Chem. 281 (2006) 26483–26490.
[9] A. Miyoshi, Y. Kitajima, S. Kido, T. Shimonishi, S. Matsuyama, K. Kitahara, K. Miyazaki, Snail accelerates cancer invasion by upregulating MMP expression and is associated with poor prognosis of hepatocellular carcinoma, Br. J. Cancer 92 (2005) 252–258.
[10] L. Sartor, E. Pezzato, I. Dell'Aica, R. Caniato, S. Biggin, S. Garbisa, Inhibition of matrix-proteases by polyphenols: chemical insights for anti-inflammatory and anti-invasion drug design, Biochem. Pharmacol. 64 (2002) 229–237.
[11] B. Wielockx, C. Libert, C. Wilson, Matrilysin (matrix metalloproteinase-7): a new promising drug target in cancer and inflammation?, Cytokine Growth Factor Rev 15 (2004) 111–115.
[12] A. Cano, M.A. Perez-Moreno, I. Rodrigo, A. Locascio, M.J. Blanco, M.G. del Barrio, F. Portillo, M.A. Nieto, The transcription factor snail controls epithelial-mesenchymal transitions by repressing E-cadherin expression, Nat. Cell Biol. 2 (2000) 76–83.
[13] E.A. Rakha, M. Tun, E. Junainah, I.O. Ellis, A. Green, Encapsulated papillary carcinoma of the breast: a study of invasion associated markers, J. Clin. Pathol. 65 (2012) 710–714.
[14] S.O. Lim, J.M. Gu, M.S. Kim, H.S. Kim, Y.N. Park, C.K. Park, J.W. Cho, Y.M. Park, G. Jung, Epigenetic changes induced by reactive oxygen species in hepatocellular carcinoma: methylation of the E-cadherin promoter, Gastroenterology 135 (2008) 2128–2140. 2140 e2121–2128.
[15] B. De Craene, G. Berx, Regulatory networks defining EMT during cancer initiation and progression, Nat. Rev. Cancer 13 (2013) 97–110.
[16] A. Miyoshi, Y. Kitajima, K. Sumi, K. Sato, A. Hagiwara, Y. Koga, K. Miyazaki, Snail and SIP1 increase cancer invasion by upregulating MMP family in hepatocellular carcinoma cells, Br. J. Cancer 90 (2004) 1265–1273.
[17] L. McInroy, A. Maatta, Down-regulation of vimentin expression inhibits carcinoma cell migration and adhesion, Biochem. Biophys. Res. Commun. 360 (2007) 109–114.
[18] J.E. Scott, I.B. Carlsson, B.D. Bavister, O. Hovatta, Human ovarian tissue cultures: extracellular matrix composition, coating density and tissue dimensions, Reprod. Biomed. Online 9 (2004) 287–293.
[19] C.B. Harley, Telomerase and cancer therapeutics, Nat. Rev. Cancer 8 (2008) 167–179.
[20] Z. Liu, Q. Li, K. Li, L. Chen, W. Li, M. Hou, T. Liu, J. Yang, C. Lindvall, M. Bjorkholm, J. Jia, D. Xu, Telomerase reverse transcriptase promotes epithelial-mesenchymal transition and stem cell-like traits in cancer cells, Oncogene 32 (2013) 4203–4213.
[21] Y. Shen, Y.W. Zhang, Z.X. Zhang, Z.H. Miao, J. Ding, hTERT-targeted RNA interference inhibits tumorigenicity and motility of HCT116 cells, Cancer Biol. Ther. 7 (2008) 228–236.
[22] N. Rufer, W. Dragowska, G. Thornbury, E. Roosnek, P.M. Lansdorp, Telomere length dynamics in human lymphocyte subpopulations measured by flow cytometry, Nat. Biotechnol. 16 (1998) 743–747.
[23] R.R. Plentz, Y.N. Park, A. Lechel, H. Kim, F. Nellessen, B.H. Langkopf, L. Wilkens, A. Destro, B. Fiamengo, M.P. Manns, M. Roncalli, K.L. Rudolph, Telomere shortening and inactivation of cell cycle checkpoints characterize human hepatocarcinogenesis, Hepatology 45 (2007) 968–976.
[24] A.L. Min, J.Y. Choi, H.Y. Woo, J.D. Kim, J.H. Kwon, S.H. Bae, S.K. Yoon, S.H. Shin, Y.J. Chung, C.K. Jung, High expression of Snail mRNA in blood from hepatocellular carcinoma patients with extra-hepatic metastasis, Clin. Exp. Metastasis 26 (2009) 759–767.
[25] J. Jou, A.M. Diehl, Epithelial-mesenchymal transitions and hepatocarcinogenesis, J. Clin. Invest. 120 (2010) 1031–1034.
[26] F. Wang, E.R. Podell, A.J. Zaug, Y. Yang, P. Baciu, T.R. Cech, M. Lei, The POT1-TPP1 telomere complex is a telomerase processivity factor, Nature 445 (2007) 506–510.
[27] B. Chen, L.A. Gilbert, B.A. Cimini, J. Schnitzbauer, W. Zhang, G.W. Li, J. Park, E.H. Blackburn, J.S. Weissman, L.S. Qi, B. Huang, Dynamic imaging of genomic loci in living human cells by an optimized CRISPR/Cas system, Cell 155 (2013) 1479–1491.
[28] B.K. Oh, H. Kim, Y.N. Park, J.E. Yoo, J. Choi, K.S. Kim, J.J. Lee, C. Park, High telomerase activity and long telomeres in advanced hepatocellular carcinomas with poor prognosis, Lab. Invest. 88 (2008) 144–152.
[29] S.E. Artandi, R.A. DePinho, Telomeres and telomerase in cancer, Carcinogenesis 31 (2010) 9–18.
[30] G.M. Shi, A.W. Ke, J. Zhou, X.Y. Wang, Y. Xu, Z.B. Ding, R.P. Devbhandari, X.Y. Huang, S.J. Qiu, Y.H. Shi, Z. Dai, X.R. Yang, G.H. Yang, J. Fan, CD151 modulates expression of matrix metalloproteinase 9 and promotes neoangiogenesis and progression of hepatocellular carcinoma, Hepatology 52 (2010) 183–196.
[31] B. Qiao, N.W. Johnson, J. Gao, Epithelial-mesenchymal transition in oral squamous cell carcinoma triggered by transforming growth factor-beta1 is Snail family-dependent and correlates with matrix metalloproteinase-2 and -9 expressions, Int. J. Oncol. 37 (2010) 663–668.